MODELLING OF AEROPLANE DYNAMICS IN EXTREME FLIGHT CONDITIONS

Christopher Sibilski
Military University of Technology
Warsaw, Poland

Abstract

This paper presents a review of the most important phenomena associated with modelling of aircraft dynamics in extreme, limited conditions. Such investigations consist of the transformations of aircraft through its functional limits and trials to resume the aeroplane to more safe and effective conditions. These investigations are characterised of set of common features, related to course near limits, estimated return possibilities and included causes of transgression such as: pilot errors, aircraft failures, purposeful of forced by situation contravention of regulations and causes of uncontrolled transgression during exploitation of aircraft in extreme situations. Investigations of aircraft dynamics in limited flight conditions make use of mathematical simulation. Dynamics of spatial controlled motion of a jet aircraft has been considered. The complete set of non-linear equations of motion has been applied in the system of co-ordinates attached to the aircraft. Some results of numerical analysis of motion dynamics are presented.

Notation

V - aircraft air speed
F - thrust
m - aircraft mass
I_X, I_Y, I_Z, I_{XZ} - aircraft moments of inertia
P_{Xa}, P_{Ya}, P_{Za} - the components of aerodynamics forces in the velocity co-ordinates
g - acceleration of gravity
L_C, M_C, N_C - the components of the moment of forces in the right-hand members of equations. of rotating motion about the centre of mass
P, Q, R - the components of the angular velocity vector of the aeroplane in the body-fixed axes
a, b - angles of attack and slip, respectively
j_s- angle of engines setting
Q, F, Y - angles of pitch, roll and yaw of the aeroplane respectively
C_L - lift coefficient
C_D - drag Coefficient
C_Y - lateral force coefficient
C_l - rolling moment coefficient
C_m - pitching moment coefficient
C_n - yawing moment coefficient
n_T, w_T - angular velocity of engines rotors

Introduction

Investigations of controlled flight of an airship in extreme flight conditions and when breaking through various limits of usage are of great cognitive and practical importance. Such investigations consist of transformations of the airship through its functional limits and trials to resume the airship to more safe and effective conditions. This produces the unique set of information about the airship behaviour, effects correlation, mutual limits configuration, enabling the aircraft with better safety and widen usage range to be designed. Investigations into the aircraft dynamics in extreme flight conditions make use of mathematical simulation.
These investigations are characterised by a set of common features, related to course near limits, estimation of return possibilities and include causes of limit transgression such as:

- Pilot errors
- Aircraft failures
- Purposeful or forced by situation in contravention of regulations and reasons for uncontrolled limit transgressions during exploitation of the aircraft in extreme situations.

Fig. 1 illustrates the possibilities of control process realised by stages 1,2,3, where several limits and areas can be characterised as follows:

- Area of normal exploitation.
- Limits and areas of hazard, when near-to-limit conditions have radically affected the airship control.
- Permissible areas of control, when after limit transgression the return to mission performance is possible with the help of special steering process.
- Area of failure when after transgression of limit the airship damage follows, but with the help of average control it is possible to return to the flight under control, but it is impossible to accomplish the mission.
- Area of catastrophe, when after transgression of limit the airship is uncontrolled and a flight ends with the crash.

Non-linear equations of motion

Non-linear equations of motion of the aeroplane and the kinematics relations will be expressed making use of moving co-ordinate systems, the common origin of which is located at the centre of mass of the aeroplane (Figs. 1 and 2) - that is, a vertical moving systems of co-ordinates $Ox_gy_gz_g$, the Oz_g axis of which is vertical and directed downwards, a system of co-ordinates $Oxyz$ attached to the aircraft, the Oxz plane coinciding with the symmetry plane of the aircraft and a system of co-ordinates attached to the air flow $Ox_ay_az_a$ in which the Ox_a axis is directed along the flight velocity vector V and the Oz_a axis lies in the symmetry plane of the aircraft and is directed downwards. The relative position of the vertical system $Ox_gy_gz_g$ and the system $Oxyz$, attached to the aircraft is described by Euler angles Q, F and Y (Fig. 2), while the relative position of the system $Oxyz$ and the system $Ox_ay_az_a$ attached to the air - by the angle of attack a and that of slip b (Fig.2). Aircraft will be considerated as a rigid body with moving elements of control surfaces. Gyroscopic moment of rotating masses of the engines will be included. Equations of motion will be leaded using Newton's principle of dynamics as well as methods of analytical mechanics (for example Boltzmann-Hammel's or Maggii's equations).

In accordance with Ref. 1, the following set of equations of motion of an aeroplane centre of mass in an explicit form in the velocity system of co-ordinates is found

$$\begin{cases} \dfrac{dV}{dt} = \dfrac{1}{m}\Big\{\Big[F\cos(\alpha+\varphi_s) - mg(\sin\Theta\cos\alpha - \\ \quad -\cos\Theta\cos\Phi\sin\alpha)\Big]\cos\beta + \\ \quad + mg\cos\Theta\sin\Phi\sin\beta - P_{X_a}\Big\} \\ \dfrac{d\alpha}{dt} = Q - (P\cos\alpha + R\sin\alpha)\tan\beta - \\ \quad - \dfrac{1}{mV\cos\beta}\Big[F\sin(\alpha+\varphi_s) - mg(\sin\Theta\sin\alpha + \\ \quad + \cos\Theta\cos\Phi\cos\alpha) + P_{Z_a}\Big] \\ \dfrac{d\beta}{dt} = P\sin\alpha - R\cos\alpha - \dfrac{1}{mV}\Big\{\Big[F\cos(\alpha+\varphi_s) + \\ \quad - mg(\sin\Theta\cos\alpha - \cos\Theta\cos\Phi\sin\alpha)\Big]\sin\beta + \\ \quad - mg\cos\Theta\cos\Phi\cos\beta - P_{Y_a}\Big\} \end{cases} \quad (1)$$

together with set of equations of the rotating motion about the centre of mass in an explicit form in the body fixed axes

$$\begin{cases} I_X\dfrac{dP}{dt} + (I_Z - I_Y)QR - I_{XZ}\left(\dfrac{dR}{dt} + PQ\right) = L_C \\ I_Y\dfrac{dQ}{dt} + (I_X - I_Z)PR + I_{XZ}(P^2 - R^2) = M_C \\ I_Z\dfrac{dR}{dt} + (I_Y - I_X)PQ - I_{XZ}\left(\dfrac{dP}{dt} - QR\right) = N_C \end{cases} \quad (2)$$

The equations of motion should be completed by the following kinematics relations which will enable us to determine the angular position of the airship relative the moving system of co-ordinates $Ox_gy_gz_g$ (Fig.2).

$$\begin{cases} \dfrac{d\Psi}{dt} = (R\cos\Phi + Q\sin\Phi)/\cos\Theta \\ \dfrac{d\Theta}{dt} = Q\cos\Phi - R\sin\Phi \\ \dfrac{d\Phi}{dt} = P + (Q\sin\Phi + R\cos\Phi)\tan\Theta \end{cases} \quad (3)$$

$$\begin{cases} \dfrac{dx_g}{dt} = u\cos\Theta\cos\Psi + \\ \quad + v(\sin\Theta\cos\Phi\cos\Psi - \cos\Phi\sin\Psi) + \\ \quad + w(\sin\Theta\cos\Phi\cos\Psi + \sin\Phi\sin\Psi) + \\ \dfrac{dy_g}{dt} = u\cos\Theta\sin\Psi + \\ \quad + v(\sin\Theta\sin\Phi\sin\Psi + \cos\Phi\cos\Psi) + \\ \quad + w(\sin\Theta\cos\Phi\sin\Psi - \sin\Phi\cos\Psi) \\ \dfrac{dz_g}{dt} = -u\sin\Theta + v\cos\Theta\sin\Phi + \\ \quad + w\cos\Theta\cos\Phi \end{cases} \quad (4)$$

The velocity components in the reference frame attached to the aircraft can be found from the equations:

$$\begin{aligned} u &= V\cos\alpha\cos\beta \\ v &= V\sin\beta \\ w &= V\sin\alpha\cos\beta \end{aligned} \quad (5)$$

The causes of motion to be study are those of flight without response of the pilot and those of controlled flight during which the control surfaces are displaced and the engine thrust varied.

Equations of motion will be complemented with equations of engines dynamics:

- equation of engines rotation.

$$n_T = K_1^T(Ma, \tau, \rho)\frac{n_{T_{max}} - n_{T_0}}{\delta_{T_{max}}}\delta_T \quad (6)$$

- equation of thrust

$$T = T_0(n_T)\left(\frac{\rho}{\rho_0}\right)^{0.7}\left(A + BMa + CMa^2\right) \quad (7)$$

- equation of gas-turbine compressor rotation

$$\omega_T = \frac{2\pi}{60}n_T \quad (8)$$

Vector of moment of the engines thrust and the gyroscopic moment of the rotating masses of engines will be found from the equation:

$$\mathbf{M}^{\mathbf{T}} = \sum_i \mathbf{M}_i^{\mathbf{T}} = \sum_i\left(\mathbf{r}_i \times \mathbf{T}_i + \mathbf{J}_{T_i}\vec{\omega}_{T_i} \times \vec{\Omega}\right) \quad (9)$$

where:

$\mathbf{r}_i$ - vectors determining the distance of the engines thrust from the centre mass of the airship;

$\mathbf{T}_i$ - vectors of the thrust;

$\mathbf{J}_{T_i}$ - the polar moments of inertia of the engines rotors;

$\vec{\omega}_{T_i}$ - vectors of angular velocity of the engines rotors;

$\vec{\Omega}$ - vector of angular velocity of the aircraft.

Aerodynamic forces and moments

The aerodynamic forces in the velocity co-ordinates can be expressed in the form:

$$P_{X_a} = \frac{1}{2}\rho V^2 S C_D$$
$$P_{Y_a} = \frac{1}{2}\rho V^2 S C_Y \qquad (10)$$
$$P_{Z_a} = \frac{1}{2}\rho V^2 S C_L$$

where S is the wing area and ρ - air density.
The aerodynamic moments in the body-fixed axes can be expressed in the form:

$$L = \frac{1}{2}\rho V^2 S l C_l$$
$$M = \frac{1}{2}\rho V^2 S b_A C_m \qquad (11)$$
$$N = \frac{1}{2}\rho V^2 S l C_n$$

where l and b_A are the span and the mean aerodynamic chord of the wing, respectively.

Qualification of the drag coefficient C_D.

The drag coefficient C_D is the following function of the angle of attack, Mach number of flight Ma and in general cause angular velocity of pitch Q, velocity of changing of angle of attack $\dot{\alpha}$ and elevator angle δ_H.

$$C_D = C_D(\alpha, Ma) + C_D^{\dot{\alpha}}\dot{\alpha} + C_D^{Q} Q + C_D^{\delta_H}\delta_H \qquad (12)$$

it is possible to assume, that:

$$C_D^{Q} = C_D^{\dot{\alpha}} = C_D^{\delta_H} \approx 0;$$

therefore:

$$C_D = \mathrm{f}(\alpha, Ma) \qquad (13)$$

Qualification of the lateral force coefficient C_Y

The coefficient of lateral force is function of:

$$C_Y = C_Y(\alpha, \beta, P, Q, R, \delta_V, \delta_E, Ma) \qquad (14)$$

where: β is a slip angle, P,Q,R are the components of the angular velocity vector of an aeroplane in body-fixed axes, δ_V, δ_E are rudder and aileron angle respectively. For low angles of attack expressions of the of coefficient of aerodynamic lateral force will be assumed in form of linear functions of: a slip angle β; components of aircraft angular velocity vector P,Q,R; angles of aileron (δ_L), rudder (δ_V) and elevator (δ_H).

Qualification of the lift coefficient C_L

The lift coefficient C_L will be assumed in the form:

$$C_L = C_L(\alpha, \dot{\alpha}, \beta, \delta_H, P, Q, R, Ma) \qquad (15)$$

For low angles of attack expression of the lift force and coefficients will be assumed in form of linear function of: an angle of attack α, a pitching angular velocity of aircraft Q and angle of elevator (δ_H).

Qualification of the rolling moment coefficient C_l

The coefficient of the rolling moment will be assumed in the form:

$$C_l = C_l(\alpha, \beta, Ma, \delta_V, \delta_L, P, Q, R) \qquad (16)$$

Qualification of the pitching moment coefficient C_m.

The coefficient of the pitching moment C_m will be assumed in the form:

$$C_m = C_m(\alpha, \dot{\alpha}, \beta, \delta_H, Ma, P, Q, R) \qquad (17)$$

Qualification of the yawing moment coefficient C_n

The coefficient of the yawing moment C_n will be assumed in form:

$$C_n = C_n(\alpha, \beta, \delta_V, \delta_L, Ma, P, Q, R) \qquad (18)$$

For low angles of attack expressions of the aerodynamic forces and moments coefficients will be assumed in form of linear functions of: a slip angle β; components of aircraft angular velocity vector P,Q,R; angles of aileron (δ_L) rudder (δ_V) and elevator (δ_H).

Influence of components of angular velocity vector of an aeroplane on rolling, pitching and yawing moments.

Aerodynamics derivatives $C_l^P, C_l^R, C_n^P, C_n^R$ will be found witch the assumption that angle of attack is low. It is mean, that $\sin\alpha \approx \alpha$ and $\cos\alpha \approx 1$. In rough estimation aerodynamic derivatives will be calculated using this method up to $\alpha \le 20^0$. When angle of attack $\alpha > 20^0$, because of nonlinearities method of finite increments was applied. The wing was divisible into sections. On elemental wing section $b \times dy$ distant from axis of rotation on y, follows increase the angle of attack $\Delta\alpha = \frac{Py}{V}$ and increase respectively C_D and C_L (Fig.4).
The rolling moment will be integral of the elementary moments of finite increments:

$$L(P) = -\frac{1}{2}\rho \int_{-\frac{l}{2}}^{\frac{l}{2}} \left(\frac{V}{\cos\Delta\alpha}\right)^2 \left[K_L(y)\left(C_L + \Delta C_L\right)\times\right. \qquad (19)$$
$$\left.\times\cos\Delta\alpha + K_D(y)\left(C_D + \Delta C_D\right)\sin\Delta\alpha\right] b(y)\, y\, dy$$

This integral will be calculated numerically:

$$L(P) = -\frac{1}{2}\rho\sum_i \left\{ \left(\frac{V}{\cos\Delta\alpha}\right)^2 \left[K_L(y_i)\left(C_L + \Delta C_L\right) \times \right.\right.$$
$$\times \cos\Delta\alpha_i + K_D(y_i)\left(C_D + \Delta C_D\right)\sin\Delta\alpha_i \Big] \times \quad (20)$$
$$\left.\left. \times b(y_i)\Delta y \right\}\right.$$

where $\Delta\alpha_i = \frac{Py_i}{V}$; y_i - distance of the item wing section from axis of rotation;
Δy_i - width of item; $b(y_i)$ - chord of item wing section, K_L - coefficient taking into consideration lift distribution along the wing span, K_D - coefficient of drag distribution along the wing span.
The yawing moment will be calculated using similar method of finite increments.

$$N(P) = \frac{1}{2}\rho\int_{-\frac{l}{2}}^{\frac{l}{2}} \left(\frac{V}{\cos\Delta\alpha}\right)^2 \left[-K_L(y)\left(C_L + \Delta C_L\right)\sin\Delta\alpha + \right.$$
$$\left. + K_D(y)\left(C_D + \Delta C_D\right)\cos\Delta\alpha \right] b(y)dy \quad (21)$$

replacing integral by addition, after division the wing into „i" sections will be received:

$$N(P) = \frac{1}{2}\rho\sum_i \left\{ \left(\frac{V}{\cos\Delta\alpha_i}\right)^2 \left[-K_L(y_i)(C_L + \right.\right.$$
$$+ \Delta C_L)\sin\Delta\alpha_i + K_D(y_i)(C_D + \Delta C_D) \times \quad (22)$$
$$\left.\left. \times \cos\Delta\alpha_i \right] b(y_i)y_i\Delta y \right\}$$

In similar manner functions $L(R)$ and $N(R)$ will be calculated. In this case the angular yawing velocity increased flow velocity ($\Delta V = Ry$) and aerodynamic moments will be equal:

$$L(R) = \frac{1}{2}\rho\int_{-\frac{l}{2}}^{\frac{l}{2}} K_L(y)C_L\left(V + Ry\right)^2 yb(y)dy \quad (23)$$

replacing integral by addition:

$$L(R) = \frac{1}{2}\rho\sum_i \left[K_L(y_i)C_L\left(V + Ry_i\right)^2 y_i b(y_i)\Delta y \right] \quad (24)$$

For yawing moment:

$$N(R) = -\frac{1}{2}\rho\int_{-\frac{l}{2}}^{\frac{l}{2}} K_D(y)C_D\left(V + Ry\right)^2 yb(y)dy \quad (25)$$

replacing integral by addition:

$$N(R) = -\frac{1}{2}\rho\sum_i \left[K_D(y_i)C_D\left(V + Ry_i\right)^2 y_i b(y_i)\Delta y \right] \quad (26)$$

Aerodynamic phenomena at high angle of attack

The following areas of flow can be distinguished as a function of angle of attack:

i. Low angles of attack: attached, symmetric, steady flow. Linear variation of aerodynamic forces and moments with α.
ii. Moderate angles of attack: separated, symmetric, rolled vortices in steady flow. Non-linear variation of aerodynamic forces and moments with α.
iii. High angles of attack: separated, symmetric, rolled vortices in steady flow, non-linear variation of forces and moments with α.
iv. Higher angles of attack: vortex break down, non-steady flow, loss of lift.
v. Very high angles of attack: non-steady turbulent wake, post stall aerodynamic characteristics.

In flow regimes i.-ii. the panel methods are successfully applied [4], [5], [6], [7]. Even for leading-edge and tip separation in the sharp edges case the prediction of the total aerodynamics loads and stability derivatives is numerically possible with good accuracy [7]. Nonlinearities are caused by crosflow and vortices shedding up from leading-edge and tip sharp edges. Primary , secondary and even tertiary vortices were observed [7]. Strong differences between results obtained from linear and non-linear Vortex Lattice Method can be observed [7]. It should be emphasised that in flow regimes described in points iii.-v. the strong nonlinearities between α and aerodynamics forces and moments can be observed. Transition from one phase to another depends on many factors (such as Reynolds Number, surface inaccuracy etc.). Description of nature of the flow at high angles of attack can be found in works of Orlik-Ruckemannn [8], [9], Rom [10] and others (for example: [11], [12], [13]). As result of non-symmetric flow on high angles of attack, significant aerodynamic cross-coupling between longitudinal and lateral response of aircraft can bee observed . This cross-coupling effects are represented by their corresponding stability derivatives (such as pitching moment due to yaw or rolling moment due to pitching [14]). Hysteresis effects were also observed [11], [15]. Experimental research has shown that cross-coupling and accelerations effects are comparable.
Many accidents of military aircraft were caused by the flight at high angles of attack, where sever degradation in handling qualities is encountered [16].

Modelling of Deep Stall Phenomenon

Term „deep stall" means phenomenon of increasing of lift coefficient C_L over the value C_{Lmax} achieved in static air-flow conditions. This phenomenon has been discovered by dint of helicopters. Designers observe that helicopters may fly with higher than resulted from restrictions due to transgression of critical angles of attack on recurring rotor blades speeds. One of the first work describing this phenomenon was published in 1967 [18]. This question has been investigated in many works. It will be discovered similar phenomena occurring on turbo-compressors and aeroplane wings. Modelling of air-flow on dynamic stall conditions belongs to very involved problems. It is not always possible or profitable to use CFD methods. Therefore dynamic stall phenomenon was a subject of many experimental works. As result of them factors affecting this phenomenon will be identificated. Taking as basis manner of utilisation of experimental data three groups of methods describing the deep stall phenomenon will be classificated[19].

I. Group of approximation methods. In this group results of experimental researches help either to calculate of airfoil loads or to estimate parameters of mathematical description (for example factors of approximation polynomial). In this group will be distinguished three methods.
   a) method of aerodynamic factors. Airfoil loads are calculated directly from experimentally assigned (in wind tunnels) aerodynamic factors;
   b) method of generalised airfoil data. Airfoils loads are calculated by help of mathematical expressions receiving on basis of approximation of aerodynamics factors measuring experimentally;
   c) analytical methods. Aerodynamic loads are calculated on basis of analytical expressions which are chosen in such manner that they describe measured experimentally process of deep stall phenomenon. An example is a procedure of calculation of aerodynamic loads of helicopter rotorblade airfoil in deep stall conditions suggested by Tarzanin [20], or methods described by Wayne [21].

II. Semi-empiricall methods which use differential equations for prediction of unsteady aerodynamic loads. The form and coefficients of this equations are determinated by technique of parameter identification. The basic model was developed by ONERA (*Office National d'Etudes et de Recherches Aerospatiales*) for loads at rotor blade section in stall conditions [22,23,24,25]. Also model of deep stall phenomenon suggested by Leischmann and Beddoes [26, 27] belongs to this method. The ONERA model assumed that aerodynamic coefficients (Lift, Drag and Pitching Moment Coefficient) incorporate a single lag term operating on the linear part of the airfoil's steady force curve, and two lag term operating on the non-linear portion of airfoil's steady force. Application of the ONERA model to unsteady aerodynamic wing model is described in Ref. 12.

III. Analytical methods, based either on the unsteady vortex lattice method (ULV) [28], or Euler and Navier-Stokes models [29], [30], [31, [32]. Probably it is not possible to use the Navier-Stokes model with the turbulence taken into account now - because of insufficient computational potential - lack of access to supercomputers of operating speed in range GFlops and memory capacity in range GB. The ULV method appeared to be appropriate to calculate unsteady loads and stability derivatives of an aeroplane an high angles of attack. The unsteady vortex lattice method, like other panel methods basing on model of potential flow, uses the Laplace's equation as mathematical description:

$$\nabla^2 \phi = 0 \qquad (27)$$

where ϕ is potential of velocity. Equation. 27 is linear, but because of non-linear boundary conditions on wake vortex , which unwind after each time steep [33] the problem is non-linear.

Numerical examples

The asymmetric drop of suspended load can be regarded as flight in the permissible or failure area [1]. Dynamics of disturbed spatial motion of an aeroplane after drop of loads has been studied, on the assumption, that the displacement of the elevator, rudder and ailerons and the engine thrust remain unchanged (uncontrolled flight) and in the case of controlled flight (the control surfaces are displaced and the thrust varied). Some results of the analysis are shown in figs. 5, 6, 7, 8 in the form of diagrams of variation of the angles of attack and slip (fig. 5), normal load factor (fig. 6) roll and pitch angles (fig. 7 and 8). It can be stated that in case of asymmetric air drop in uncontrolled horizontal flight considerable variation in all the flight parameters occurs.

The accident of the fighter aircraft Su-22M4 can be regarded as example of forced by situation limit transgression. When performing the group flying over the firing ground (vee formation of aircraft) , pilot of second aircraft rapidly pulled the stick and deflected the rudder (because of danger of collision). Such pilot's activity caused stall of the aircraft. Because of low flight altitude pilot had to catapult. Some results of numerical simulation of this accident are shown on figs. 9, 10, 11. Fig. 11 pictured deflection of control surfaces (reconstruction of pilot's activity). Fig. 9 shown diagram of variation of angle of attack α and

normal load factor n_z . Fig. 10 pictured variation of airspeed and altitude.
Spin of the aircraft can be regarded as the example of flight in permissible area of control (fig. 1).
Some results of numerical simulation of spin of training-combat aircraft are shown in figs. 12, 13, 14, 15, 16 in form of diagrams of variation of normal load factor n_z (fig. 12), angular velocities P, Q, R (fig. 13), airspeed (14), flight altitude (fig.15) and deflection of control surfaces (fig. 16).
Reconstruction and simulation of the time dependent flight path for the aircraft accident are describe in terms a process known as forensic engineering. Forensic engineering consists in application of the scientific and engineering knowledge to legal matters, such as accident reconstruction. The sample issue of forensic engineering is the reconstruction of flight dynamics of an aeroplane having damaged the elevator unit. This case may be the example of flight analysis in failure conditions. Making use of the results of the analysis it can be asserted that a motion of the aeroplane with damaged tail unit is stirringly influenced by stabiliser set-up and there is a possibility of avoiding the aeroplane crash on condition that the pilot is acting in appropriate way [34]. Figs. 17, 18, 19 show the results of numerical reconstruction of crash of the W300 training-combat aircraft in Radom on January 30, 1987. The analysis of crash, supplied with numerical simulation has been carried out, taking into consideration both the way of deconstruction and arrangement of wreckage as well as available parts of records made by flight parameters and vibration registers. Flutter of the tail plane was responsible for this crash [35], [36]. Figs. 20, 21, 22, 23 show results of numerical reconstruction of training aircraft crash. The numerical analysis of crash has been carried out, taking into consideration records made by automatic flight recorder, just before the catastrophe. Fig. 20 shows variation of normal load factor n_z, fig. 20 pictures variation of angular velocities P, Q, R, figs. 22 and 23 show variation of pitch angle Θ and roll angle Φ. Before the crash aircraft roll realising two and half turns (in the time 10 sec.). After that time pilot turn the aircraft from invert flight into straight flight. During the rolls follows change of longitudinal decalage of tail plan („Bob-weight" effect on the elevator control system). This causes very high force on the stick and uncontrollable fall down of the normal load factor (fig. 20). The crash of the aircraft was as result of them.
An example of flight in the permissible area of control is flight in deep stall conditions. The manoeuvre „Cobra" will be realised in deep stall conditions. Figs. 24, 25, 26 show variation of selected flight parameters in this manoeuvre [37].

References

1. Dżygadło Z., Sibilski K., "Dynamics of Spatial Motion of an Aeroplane After Drop of Loads", J. of Tech. Phys., Warsaw, Vol. 29, No 3-4, 1988.

2. Dżygadło Z., Kowaleczko G., Sibilski K., "Aerodynamic Characteristics of the Aeroplane with Strake Wing and its Natural Motions", Rep. of Inst. of Aviation No. 136, 1994 (in Polish).

3. Szumański K., „Transgressions in a pilot-helicopter system", Rep. of Inst. of Aviation No. 126-127, 1991 (in Polish).

4. Hedman S. G.,"Vortex Lattice Method for Calculation of Quasi Steady State Loadings on Thin Elastic Wings", Rep. 105, Oct. 1965, Aeronautical Research Institute of Sweden.

5. Katz J., Platkin A.,"Low -Speed Aerodynamics. From Wing Theory to Panel Methods", McGraw-Hill, N.Y. 1991.

6. Goraj Z., Piertucha J., „Panel methods: a routine tool for aerodynamic calculations: the state-of-the-art", J. of Theor. and Appl Mech., 1993

7. Kandil O. A., Mook D. T., „Non-linear Prediction of Aerodynamic Load on Lifting Surfaces", J. of Aircraft, vol. 13, No 1, Jan. 1976.

8. Orlik-Ruckemann K. J.,"Aerodynamic Coupling Between Lateral and Longitudinal Degrees of Freedom"; AIAA Journal, vol. 15, No.12, Dec. 1977.

9. Orlik-Ruckemann K., J.,"Aerodynamic Aspects of Aircraft Dynamics at High Angles of Attack", J. of Aircraft, vol.20,No.9, Sept. 1983.

10. Rom J.,"High Angle of Attack Aerodynamics, Subsonic, Transonic and Supersonic", Springer-Verlag, 1992.

11. Lowsn M. V., Ponton A. J.,"Symmetry Breaking in Vortex Flows on Conical Bodies", AIAA Journal vol. 30, No.6., June 1992.

12. Meijer J. J ., Cunningham A. M. Jr., „Outline and Applications of a Semi-Empirical Method for Predicting Transonic Limit Cycle Oscillation Characteristics of Fighter Aircraft", The Royal Aeronautical Society International Forum on Aeroelasticity and Structural Dynamics, Manchester, England, 26-28 June 1995.

13. Modi V. J., Cheng C. W., Mak. A., Yokimiza T.,"Reduction of side force on pointed bodies

through add-on tip devices", AIAA Journal, vol. 30, No. 10., Oct. 1992.

14. Orlik-Ruckemann K.J., Hanf E. S., „Experiments on cross-coupling and translational accelerations derivatives", AGARD-CP-235, Paper 8, 1978.

15. Tobak. M., Shiff L. B.,"Aerodynamic Mathematical Modelling Basic Concepts", AGARD-LS-114, Lecture 1, 1981.

16. Tiriga A. Jr., Ackerman J. S., Skow A. M., "Design Technology for Departure Resistance of Fighter Aircraft"; AGARD-CP-199, Nov. 1975.

17. Hounjet M. H. L.,"A Field Panel/Finite Difference Method for Potential Unsteady Transonic Flow", AIAA Journal., vol. 23, No.4, April 1985.

18. Harris F., Pruyn R., „Blade Stall of Helicopter - Half Fact, Half Fiction", 23-rd Annual National Forum of Amer. Helic. Soc., May 1967.

19. Narkiewicz J., „Rotorcraft Aeromechanics and Aeroelastic Stability". Sci. Works of Warsaw Univ. of Tech., Mech. vol. 158, 1994.

20. Tarzanin F., J., „Prediction of Control Loads Due Stall", 27th Annual National V/STOL Forum of the Amer. Helicopter Soc., May 1971.

21. Wayne J., „Comparison of Three Methods for Calculation of Helicopter Blade Loading and Stress Due Stall", NASA TN D-7833, Washington DC, Nov. 1974.

22. Dat R., Tran C. T., Petot D., „Modele Phenomenologique de Decrochage Dynamique sur Profil de Pale d'Helicoptere", ONERA T. P. No. 1979-149.

23. Tran C. T., Petot D., „Semi-Empirical Model for the Dynamic Stall of Airfoils in View of the Application to the Calculation of Responses of a Helicopter Rotor Blade in Forward Flight", Vertica, Vol. 5, 1981.

24. Mc.Alister K. W., Lambert O., Petot D., „Application of the ONERA Model of Dynamic Stall", NASA TP2399 or AVSCOM TP84-A-3, 1984.

25. Narkiewicz J., Syryczyński J, Batler T., „Circulation ONERA Model for Dynamic Airfoil Stall", Works of Institute of Aviation, vol. 1-2, No 132-133, 1993.

26. Leishman J. G., Beddoes T. S., „A Semi-Empirical Model of Dynamic Stall", Journal of Amer. Helic. Soc. vol. 34/5, Oct. 1990.

27. Leischman J. G., Nguen K. G., „State-Space Representation of Unsteady Airfoil Behaviour", AIAA Journal, vol. 28 no. 5, 1990.

28. Konstadinopoulos P. A. et al., „A Vortex-Lattice Method for General Unsteady Aerodynamics", J. Aircraft, vol. 22, No. 1, 1985.

29. Rausch R. D., Batina J. T., Yang H. T. Y., „Euler Flutter Analysis of Airfoils Using Unstructured Dynamic Meshes", J. Aircraft, vol. 27, no. 5, 1990.

30. Guruswamy G. P., „Unsteady Aerodynamic and Aeroelastic Calculations for Wings Using Euler Equations", AIAA Journal, vol. 28, no. 3, 1990.

31. Schuster D. M., Vadyak J., Atta E., „Static Aeroelastic Analysis of Fighter Aircraft Using a three-dimensional Navier-Stokes Alghoritm", J. Aircraft, vol. 27, no. 9, 1989.

32. Rizk Y. M, Gee K., „Unsteady Simulation of Viscous Flowfield Around F-18 Aircraft at Large Incidence", J. Aircraft, vol. 29, 1992.

33. Goraj Z., Pietrucha J., „Modifications of Potential Flow Model, for Improving of Panel Methods", Rep. of Inst. of Aviation, vol. 135, 1993.

34. Dżygadło Z., Sibilski K., „ Analysis of Aircraft Flight Dynamics After Damage of the Tail Plane", Bulletin of Military Univ. of Tech., vol. 40, No. 11, Nov. 1990. (in Polish)

35. Dżygadło Z., Sibilski K., „Modelling of Dynamics of Spatial Motion of an Aeroplane After Damage of the Elevator Unit", Mech. in Aviation, Polish Soc. of Theoretical and Appl. Mech., Warsaw, 1992 (in Polish)

36. Maryniak J., „Technical Aspects of the I-22 „IRYDA" Prototype Crash Analysis in Terms of the Flutter Experiments in Flight: Modelling and Numerical Simulation", Wydanie Specjalne Sympozjum „Modelowanie w Mechanice", Gliwice 1995 (in Polish).

37. Dżygdło Z., Kowaleczko G., Sibilski K., „Method of Control of Aircraft with Strake Wing During Cobra Maneuver", Zeszyty Naukowe Politechniki Rzeszowskiej, Mechanika Nr. 45; 1995 (in Polish).

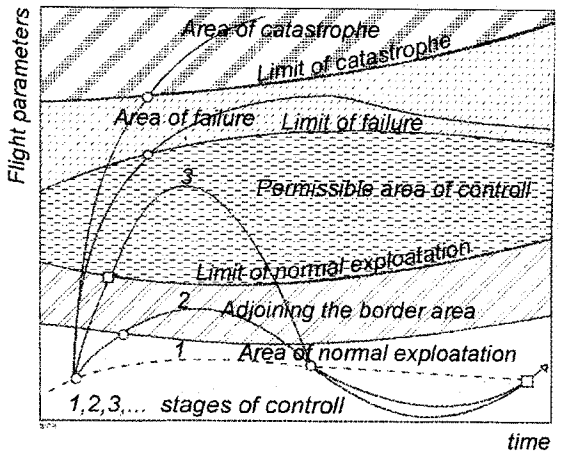

Fig. 1 Areas and limits of control process

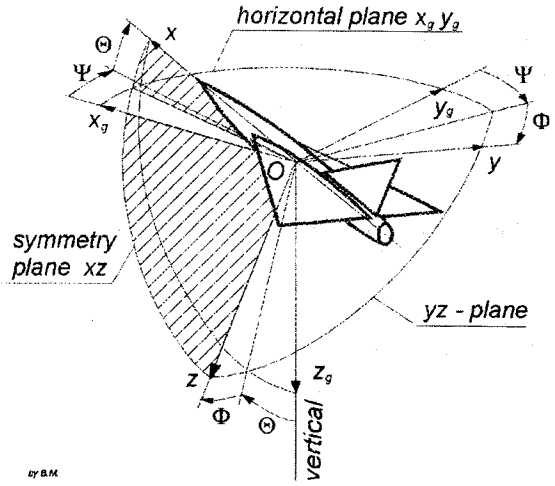

Fig. 2 System of co-ordinates attached to the aircraft

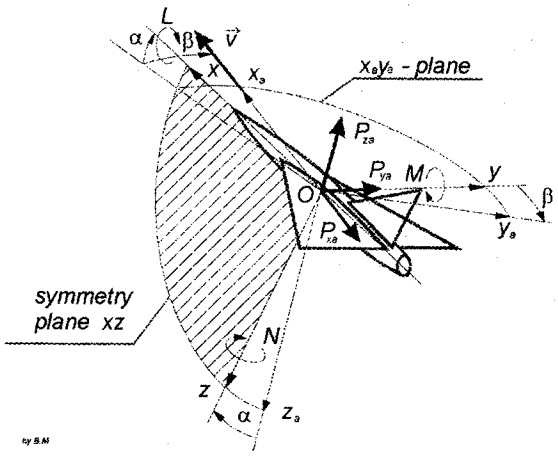

Fig. 3 System of co-ordinates attached to the airflow

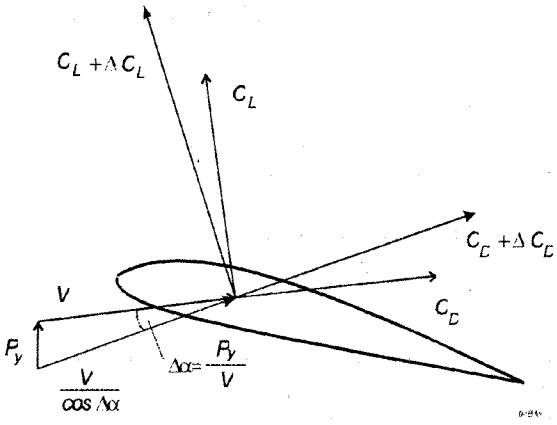

Fig. 4 The components of velocity vector and aerodynamic coefficients on a wing section

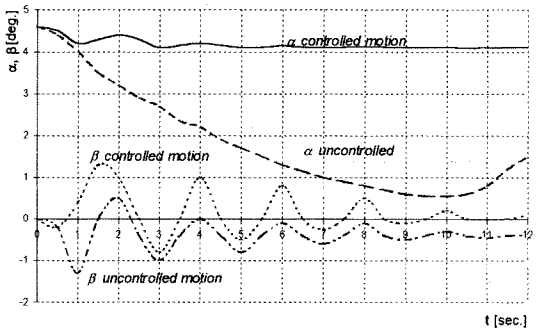

Fig. 5 Airdrop, controlled and uncontrolled flight - variation of angles of attack α and slip β

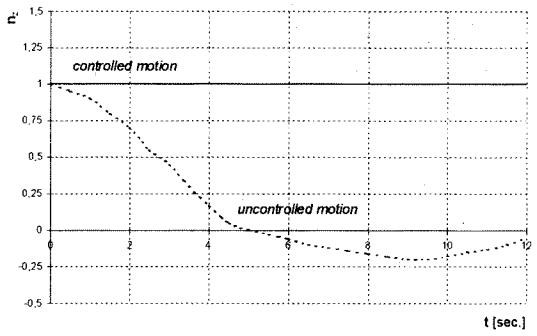

Fig. 6 Airdrop, controlled and uncontrolled flight - variation of normal load factor n_z

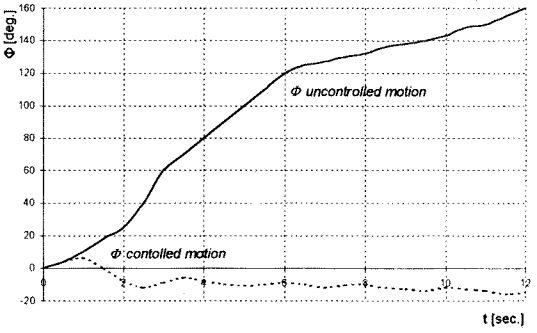

Fig. 7 Airdrop, controlled and uncontrolled flight - variation of roll angle Φ

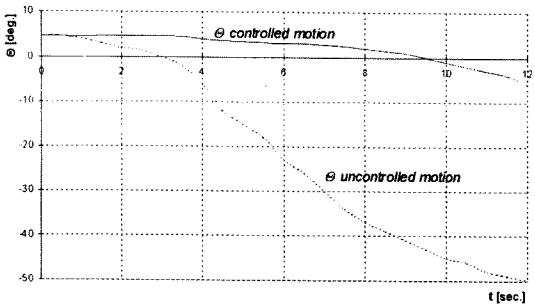

Fig. 8 Airdrop, controlled and uncontrolled flight - variation of pitch angle Θ

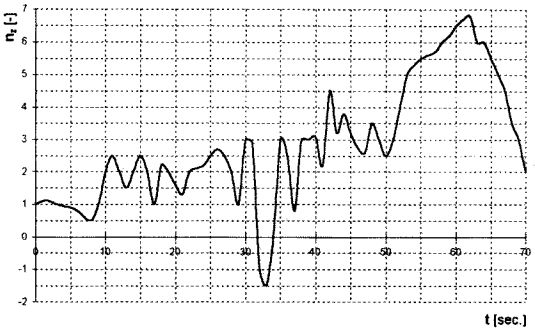

Fig. 12 Spin - variation of normal load factor n_z

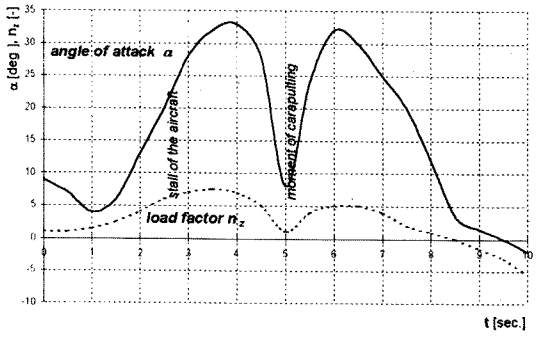

Fig. 9 Stall of the aircraft Su-22M4 - variation of angle of attack α and normal load factor n_z

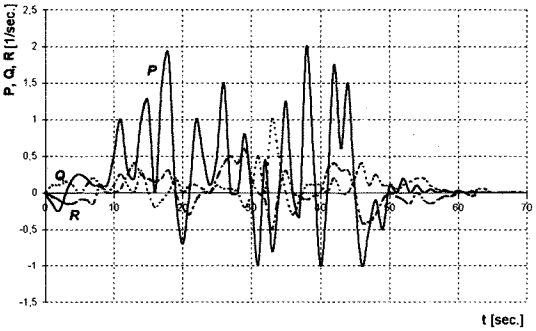

Fig. 13 Spin - variation of angular velocities P,Q,R

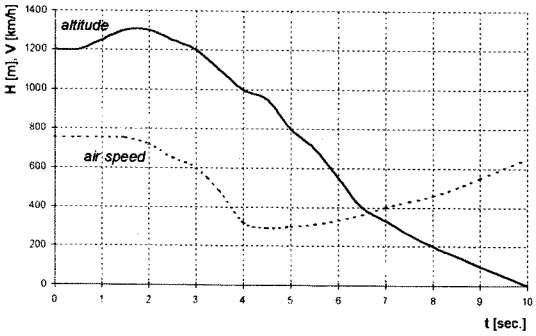

Fig. 10 Stall of the aircraft Su-22M4 - variation of airspeed and attitude

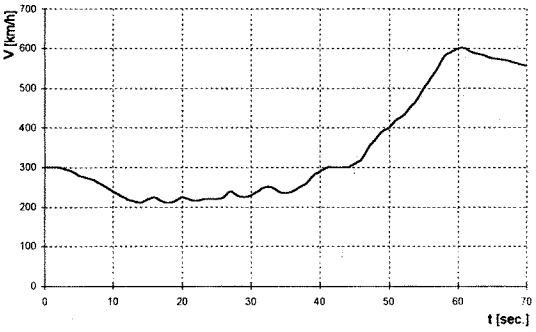

Fig. 14 Spin - variation of air speed V

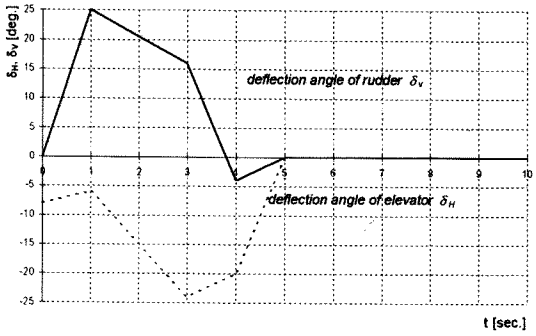

Fig. 11 Stall of the aircraft Su-22M4 - variation of angles of elevator δ_H and rudder δ_V

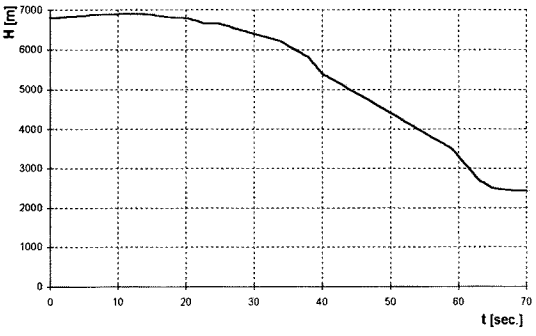

Fig. 15 Spin - variation of flight altitude H

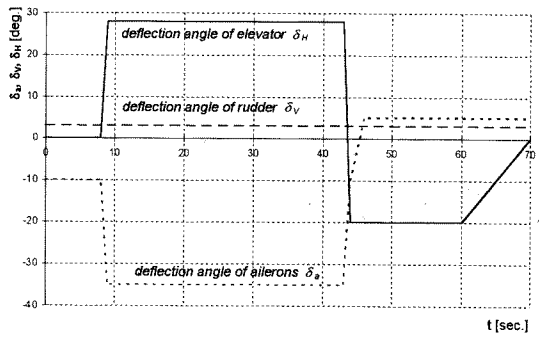

Fig. 16 Spin - deflection of control surfaces

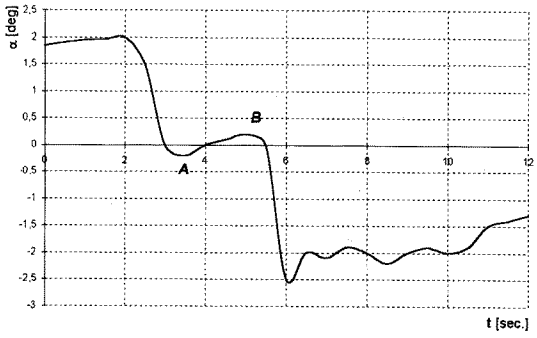

Fig. 17 The analysis of the W-300 training-combat aircraft crash - variation of angle of attack α

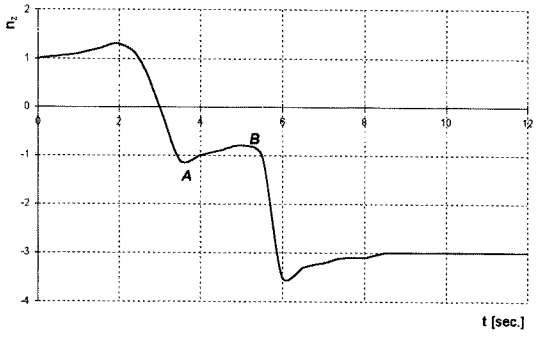

Fig. 18 The analysis of the W-300 training-combat aircraft crash - variation of normal load factor n_z

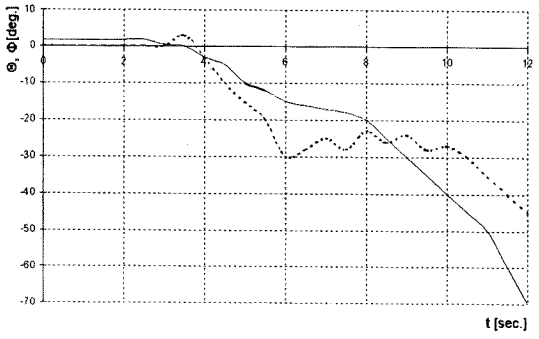

Fig. 19 The analysis of the W-300 training-combat aircraft crash- variation of pitch and roll angles

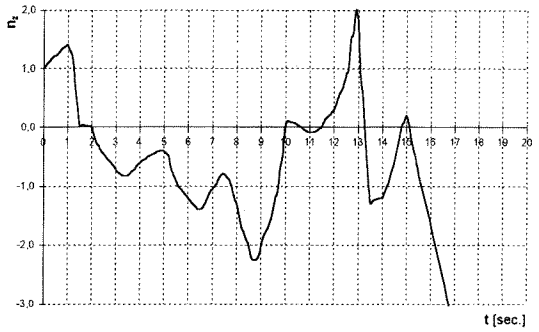

Fig. 20 Analysis of training aircraft crash - variation of normal load factor n_z

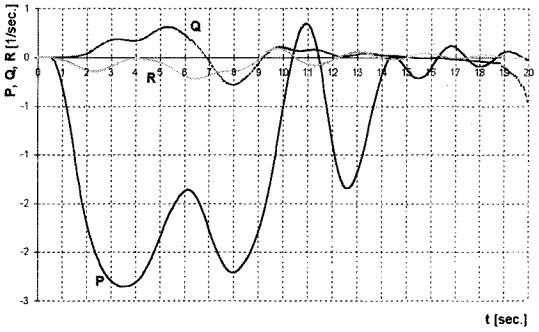

Fig. 21 Analysis of training aircraft crash - variation of angular velocities P, Q, R

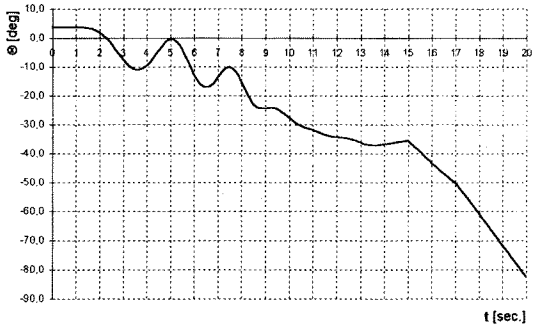

Fig. 22 Analysis of training aircraft crash - variation of pitch angle Θ

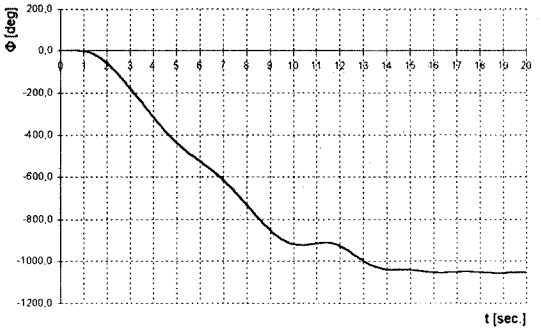

Fig. 23 Analysis of training aircraft crash - variation of roll angle Φ

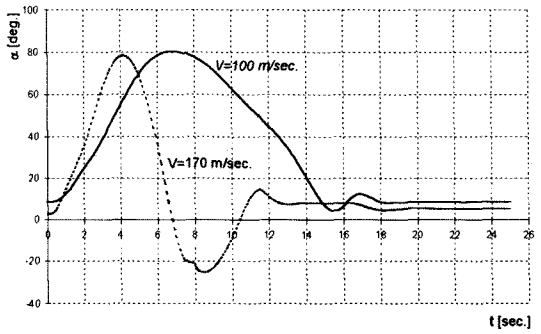

Fig. 24 „Cobra" - variation of angle of attack α

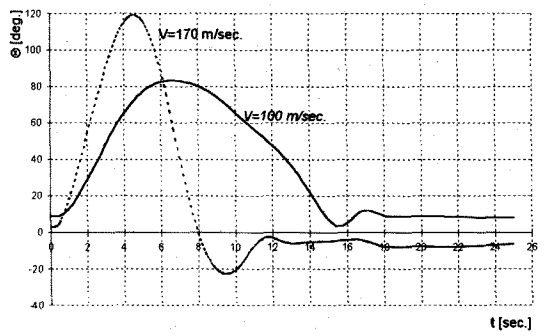

Fig. 25 „Cobra" - variation of pitch angle Θ

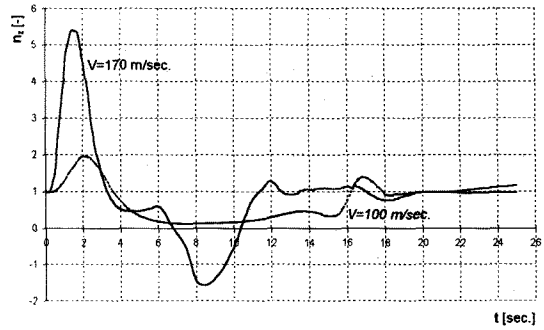

Fig. 26 „Cobra" - variation of normal load factor n_z